Nuclear spin-spin coupling in $La_{2-x}Sr_xCuO_4$ studied by stimulated echo decay

S. Fujiyama,* M. Takigawa, and Y. Ueda
The Institute for Solid State Physics, The University of Tokyo, Roppongi, Minato-ku, Tokyo 106-8666, Japan

T. Suzuki and N. Yamada
Department of Applied Physics and Chemistry, University of Electro-Communications, Tokyo 182-8585, Japan
(Received 20 April 1999)

We have performed copper nuclear quadrupole resonance experiments in high-temperature superconductors $YBa_2Cu_4O_8$, $YBa_2Cu_3O_7$, and $La_{2-x}Sr_xCuO_4$ ($x=0.12$ and $x=0.15$), using the stimulated echo technique which utilizes the rf-pulse sequence $\pi/2-(\tau)-\pi/2-(T-\tau)-\pi/2$. The τ and T dependences of the stimulated echo intensity is analyzed by a model that includes the spin-lattice relaxation process (T_1 process) and the fluctuating local field due to nuclear spin-spin coupling. The model gives quantitative account of the experimental results in $YBa_2Cu_4O_8$ and $YBa_2Cu_3O_7$, using the known values of $1/T_1$ and $1/T_{2G}$, the Gaussian decay rate of the spin-echo intensity. The same model applied to $La_{2-x}Sr_xCuO_4$ enables us to extract the value of T_{2G}. Our results indicate that T_1T/T_{2G}^z shows significant temperature dependence for $z=2$ but is approximately independent of temperature for $z=1$. This implies that the dynamic exponent is close to one in $La_{2-x}Sr_xCuO_4$. [S0163-1829(99)07137-4]

I. INTRODUCTION

Anomalous spin dynamics in high-temperature superconductors continues to be a controversial issue.[1,2] In all high-T_c materials, the dynamic susceptibility $\chi(q,\omega)$ at low frequencies is peaked near or at the antiferromagnetic wave vector $Q=(\pi,\pi)$ above T_c. The nuclear spin-lattice relaxation rate $(1/T_1)$ at the planar ^{63}Cu sites measured by NMR/NQR (nuclear quadrupole resonance) has been used extensively to probe the low-frequency spin fluctuations through the following relation:[3]

$$\frac{1}{T_1T}=\frac{\gamma_n^2k_B}{\mu_B^2}\sum_q F_\perp(q)^2\chi''(q,\omega_n)/\omega_n, \qquad (1.1)$$

where γ_n is the nuclear gyromagnetic ratio, ω_n is the nuclear resonance frequency, and $F_\perp(q)$ $(F_\parallel)$ is the Fourier component of the hyperfine coupling perpendicular (parallel) to the crystalline c axis, which is assumed to be the quantization axis of nuclear spins as is the case for NQR. It was found that $1/(T_1T)$ shows contrasting temperature dependence for different regions of doped hole concentration. For sufficiently high hole concentration, $1/(T_1T)$ keeps increasing as temperature is lowered down to T_c. In contrast, in many underdoped materials, where the hole concentration is smaller than the optimum value for highest T_c, $1/(T_1T)$ show a broad maximum at a temperature T_s, which is much higher than T_c, and decrease steeply at lower temperatures. This suggests that a pseudogap opens in the spin excitation spectrum near (π,π) above T_c.[4] As the hole concentration increases, T_s decreases. The pseudo-spin-gap phenomenon is observed in various underdoped materials, such as $YBa_2Cu_3O_{6.63}$,[5] $YBa_2Cu_4O_8$,[6] $LaBa_2Cu_3O_{7-\delta}$,[7] and $HgBa_2Ca_{n-1}Cu_nO_{2n+2+\delta}$ $(n=1,2)$.[8,9]

However, one typical high-T_c system, $La_{2-x}Sr_xCuO_4$ (LSCO) does not show clear pseudo-spin-gap behavior.[10] Instead, recent precise measurements of $1/(T_1T)$ up to 800 K (Refs. 11–13) revealed a modest change of behavior at a temperature T^*. Above T^*, $1/(T_1T)$ follows a Curie-Weiss temperature dependence, $1/(T+\theta)$. Below T^*, $1/(T_1T)$ keeps increasing but is slightly suppressed from the extrapolation of the high-temperature Curie-Weiss law. Dependence of T^* on the hole concentration is similar to that of T_s in other underdoped high-T_c materials. At present, origin of this crossover temperature or the reason for the different behavior between LSCO and other high-T_c materials is not well understood.

NQR experiments in LSCO are complicated due to large inhomogeneous linewidth of a few MHz. Since Cu spins are excited over a few hundred kHz by typical rf pulses, only a small portion of the entire Cu spins contributes to the NQR signal at one frequency. In our previous work, it was found that $1/T_1$ measured by Cu NQR is not uniform over the broad spectrum. The frequency dependence of $1/T_1$ is more pronounced in more underdoped materials,[12] indicating substantial inhomogeneity of the microscopic electronic state. One concern is that the measured value of $1/T_1$ might be influenced by the spectral diffusion process, in which Zeeman energy $\hbar\gamma_nI_zH$ of the excited nuclear spins diffuses in frequency over inhomogeneously broadened spectrum by the transverse component of nuclear spin-spin coupling of the form $aI_{i+}I_{j-}$. If this is the case, the measured value of $1/T_1$ would be larger than the true relaxation rate due to electronic spin fluctuations.

Another issue is that one cannot obtain the strength of nuclear spin-spin coupling from measurements of the spin-echo decay rate for such a broad spectrum. In cuprates, Cu nuclear spins are coupled dominantly by the Ruderman-

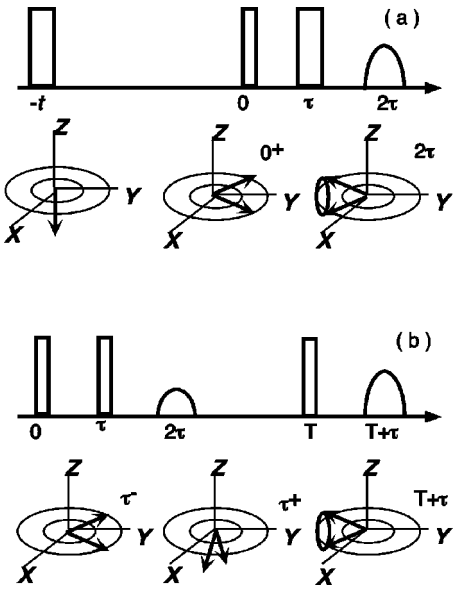

FIG. 1. Time charts of three rf pulses and corresponding states of nuclear spins in the rotating frame for (a) inversion recovery and (b) stimulated echo decay sequences.

Kittel-Kasuya-Yosida (RKKY)-type indirect interaction mediated by electronic spin excitations,

$$\mathcal{H}=\hbar\sum_{\langle ij\rangle}\{a_{\parallel}^{ij}I_{iz}I_{jz}+a_{\perp}^{ij}/2(I_{i+}I_{j-}+I_{i-}I_{j+})\}, \quad (1.2)$$

where the coupling constant is given in terms of the q-dependent static susceptibility as

$$a_{\alpha}^{ij}=\frac{1}{\hbar(g\mu_B)^2}\sum_{q}|F_{\alpha}(q)|^2\chi(q)\exp(-iqR_{ij}). \quad (1.3)$$

The large anisotropy $F_{\parallel}(q)/F_{\perp}(q)\sim 6$ for $q\sim(\pi,\pi)$ makes $a_{\parallel}$ much larger than $a_{\perp}$. Then the Gaussian time constant of spin-echo decay $1/T_{2G}$ in ^{63}Cu NQR experiments is given as[14–16]

$$\left(\frac{1}{T_{2G}}\right)^2=\frac{0.69}{4}\sum_{j\neq i}(a_{\parallel}^{ij})^2$$
$$=\frac{0.69}{4\hbar^2}\frac{1}{(g\mu_B)^4}$$
$$\times\left[\sum_{q}F_{\parallel}(q)^4\chi(q)^2-\left(\sum_{q}F_{\parallel}(q)^2\chi(q)\right)^2\right], \quad (1.4)$$

where 0.69 is the natural abundance of ^{63}Cu nucleus. Measurements of $1/T_{2G}$ have provided valuable information regarding the enhancement of the static susceptibility near the antiferromagnetic wave vector in many high-T_c materials such as $YBa_2Cu_3O_{7-\delta}$ (Y1237, $T_c\sim 90$ K),[17,18] $YBa_2Cu_3O_{6.62}$ ($T_c\sim 60$ K),[15] and $YBa_2Cu_4O_8$ (Y1248, $T_c\sim 80$ K).[18] However, Eq. (1.4) assumes that the nuclear spins over the entire spectrum are flipped by the π pulse, a condition that is not satisfied in LSCO.

In this paper, we report the results of stimulated echo[19] decay measurements in $YBa_2Cu_4O_8$, $YBa_2Cu_3O_7$, and $La_{2-x}Sr_xCuO_4$ ($x=0.12$ and $x=0.15$), using NQR at zero magnetic field. Stimulated echo sequence utilizes three $\pi/2$ pulses separated in time by τ and $T-\tau$. The decay of stimulated echo intensity as a function of T can be caused not only by the spin-lattice relaxation process but also by the spectral diffusion[20] as well as the nuclear spin-spin coupling.[21] The dependence on τ and T of the stimulated echo intensity is compared with the calculation based on a model which takes account of the spin-lattice relaxation process and the nuclear spin-spin coupling along the c axis. The effects of spin-spin coupling perpendicular to the c axis, which is much smaller than the coupling along the c axis but responsible for the spectral diffusion, is neglected as we discuss in detail below. For $YBa_2Cu_4O_8$ and $YBa_2Cu_3O_7$, where the values of $1/T_1$ and $1/T_{2G}$ are known, the calculation shows good quantitative agreement with the experimental data. The same model applied to LSCO enables us to extract the value of $1/T_{2G}$. Our results indicate that T_1T/T_{2G}^z shows significant temperature dependence for $z=2$ but is approximately independent of temperature for $z=1$. This implies that the dynamic exponent is close to 1 in $La_{2-x}Sr_xCuO_4$.

II. SAMPLE PREPARATIONS

We used polycrystalline materials synthesized by the usual solid-state reaction. For Y1248 material, we used hot-isostatic-pressing (HIP) technique. All samples were confirmed to be single phase by powder x-ray-diffraction measurements. The superconducting transition temperatures (T_c) are 90 K (Y1237), 80 K (Y1248), 38 K (LSCO $x=0.15$), and 32 K (LSCO $x=0.12$), respectively.

III. STIMULATED ECHO METHOD

We briefly discuss the stimulated echo method in comparison with the ordinary spin-echo and inversion recovery methods. In ordinary spin-echo experiments, two rf pulses ($\pi/2$ and π pulses) are applied with time separation τ. The τ dependence of spin-echo intensity is described by two parameters, $1/T_{2L}$ and $1/T_{2G}$, as[17]

$$M(2\tau)=M_0\exp\left(-\frac{2\tau}{T_{2L}}\right)\exp\left(-\frac{(2\tau)^2}{2T_{2G}^2}\right). \quad (3.1)$$

The Lorenzian component $1/T_{2L}$ represents the contribution from the spin-lattice relaxation process.[22] The Gaussian component $1/T_{2G}$ is due to nuclear spin-spin coupling and given by Eq. (1.4).

The pulse sequence for the stimulated echo experiments are described as $[\pi/2-\tau-\pi/2-(T-\tau)-\pi/2]$, which is shown in Fig. 1(b) and compared with the conventional inversion recovery sequence ($\pi-T-\pi/2-\tau-\pi$) in Fig. 1(a). The figures below the time chart of rf pulses show the corresponding state of nuclear spins in the rotating frame. In the inversion recovery sequence (a), the nuclear magnetization along the z direction initially at the thermal equilibrium is inverted by the first π pulse. The z component of the magnetization M_z, which then begins to recover toward the thermal equilibrium, is measured by the intensity of the spin-

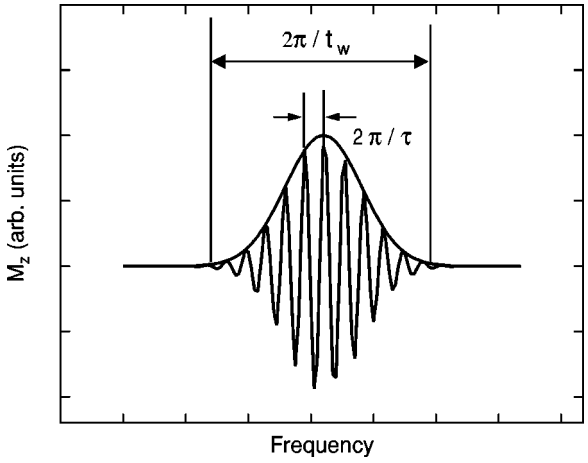

FIG. 2. Distribution of M_z in the inhomogeneously broadened spectrum in stimulated echo experiments after the second pulse. Typical values of the t_w ($\pi/2$ pulse width) and τ are 1.5 and 30 μs.

echo signal formed by the second and the third pulses. In case of NQR of ^{63}Cu nuclei ($I=3/2$), the recovery of spin-echo intensity is described by an exponential function if the effect of spectral diffusion is neglected,

$$M(T)=M_0\left[1-2\exp\left(-\frac{3T}{T_1}\right)\right], \tag{3.2}$$

where T_1 is the time constant for high-field NMR experiments.

In the stimulated echo sequence (b), the initial magnetization is flipped into the y direction by the first $\pi/2$ pulse. Then it dephases in the xy plane by the inhomogeneous distribution of the resonance frequency, as well as by the nuclear spin-spin coupling. The magnetization spread in the xy plane is flipped into the xz plane by the second $\pi/2$ pulse. The value of M_z immediately after the second pulse is given by the ensemble average of $-\cos\phi(\tau)$, where $\phi(\tau)=\gamma_n\int_0^\tau h(t)dt$ is the accumulated phase in the xy plane of individual spins subject to the local field $h(t)$ during the period between the first and second pulses. If the local-field distribution is dominated by the static inhomogeneity of the resonance frequency, M_z should be oscillating as $-\cos(\tau\omega)$ as a function of frequency over the spectrum as shown in Fig. 2. If M_z does not change between the second and the third pulse, the oscillating magnetization distribution along the z direction is flipped into the y direction by the third pulse, which then refocuses along the $-y$ direction at $T+\tau$, forming the stimulated echo. The echo intensity is given by the ensemble average of $(1/2)\cos\phi(T+\tau)$, where

$$\phi(T+\tau)=\gamma_n\int_0^\tau h(t)dt-\gamma_n\int_T^{T+\tau}h(t)dt \tag{3.3}$$

is the accumulated phase at $T+\tau$. The accumulated phase is zero if $h(t)$ is static.

Temporal variation of M_z or $h(t)$ causes the intensity of stimulated echo to decay as a function of T. Change of M_z can be caused either by the spin-lattice relaxation process (T_1 process) or by the spectral diffusion. By the T_1 process M_z recovers towards the uniform thermal equilibrium magnetization. The stimulated echo decay by the T_1 process is simply given by $\exp(-3T/T_1)$ similar to the inversion recovery.

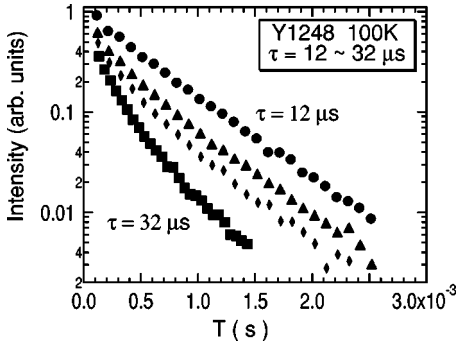

FIG. 3. Stimulated echo intensity is plotted against T for various values of τ for $YBa_2Cu_4O_8$ at 100 K.

The spectral diffusion can be caused by the transverse component of the nuclear spin-spin coupling, the second term of Eq. (1.2), which describes the mutual flip of two nuclear spins. We discuss this in more detail in the next section. The oscillating distribution of M_z will be averaged out by the spectral diffusion, leading to reduction of the stimulated echo intensity.

Stimulated echo decay is also caused by the temporal fluctuation of $h(t)$, since the two terms in the accumulated phase Eq. (3.3) then do not cancel exactly. In our NQR experiments, distribution of the local field is largely due to inhomogeneity of the electric-field gradient, which is static. However, the longitudinal component of the spin-spin coupling, the first term of Eq. (1.2), gives rise to an additional source of the local field. This local field at ith site is given as

$$h_i(t)=\frac{1}{\gamma_n}\sum_{j\neq i}a_\parallel^{ij}I_{jz}(t), \tag{3.4}$$

which fluctuates via the T_1 process.

IV. EXPERIMENTAL RESULTS AND ANALYSIS

The stimulated echo intensity M was measured as a function of T for several different values of τ. The experimental results are shown in Figs. 3 and 4 for Y-based compounds and Fig. 5 for the LSCO $x=0.12$ sample. Generally, the echo decay curve $M(T)$ deviates from a single exponential function $\exp(-3T/T_1)$. The deviation is not clearly noticed for

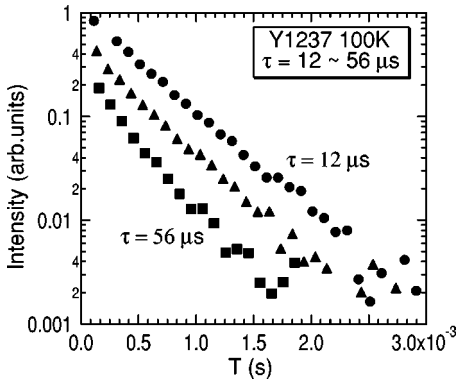

FIG. 4. Stimulated echo intensity for $YBa_2Cu_3O_7$ at 100 K.

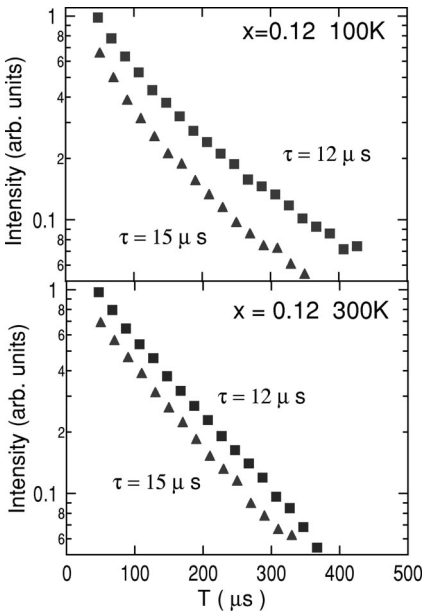

FIG. 5. Stimulated echo intensity for $La_{2-x}Sr_xCuO_4$ $x=0.12$ sample at 100 K (above) and at 300 K (below).

small τ but becomes significant for larger τ. The decay rate $d\ln M(T)/dT$ shows strong τ dependence for small T, where it is larger for larger τ. In contrast, the decay rate depends less on τ for larger T region. How strongly the decay curve changes with τ depends on temperature as well as materials. As shown in Figs. 3, 4, and 5, the τ dependence of stimulated echo decay curves become negligible at higher temperatures. At lower temperatures, the τ dependence of decay curves is most significant in the Y1248 sample.

As mentioned in the previous section, we have to consider three distinct processes for the stimulated echo decay, namely, the T_1 process, spectral diffusion, and local-field fluctuations. Of these, contribution from the T_1 process is easily separated by dividing the experimental data of stimulated echo decay by $\exp(-3T/T_1)$.

Portis has analyzed the spectral diffusion process in electron paramagnetic resonance of F centers, where diffusion occurs via the dipolar interaction between electron spins within the spectra broadened by the hyperfine interaction with surrounding nuclear spins.[23] We apply this analysis to the present problem. First, the inverse life time of the z component of a nuclear spin due to mutual spin flip of I_i and a nearby spin I_j described by the second term of Eq. (1.2) is given by[23]

$$\frac{1}{\tau_s}=0.69\times\frac{\pi}{4}f(\omega)\sum_j\,(a_\perp^{ij})^2, \tag{4.1}$$

where $f(\omega)$ is the NQR spectral shape function normalized so that $\int f(\omega)d\omega=1$ and we assume that the resonance frequencies of two neighboring nuclear spins are uncorrelated. Although the total Zeeman energy has to be conserved, the uncertainty principle allows the resonance frequencies of I_i and I_j to be different by an amount comparable to $1/\tau_s$. Thus the mutual spin flip process describes a one-dimensional random walk of magnetic particles along the frequency axis, where both the hopping rate and the hopping distance are given by $1/\tau_s$. Therefore the time evolution of the macroscopic magnetization distribution is given by a diffusion equation with the diffusion constant $D_\omega=1/\tau_s^3$. We can estimate $1/\tau_s$ as follows. From Eq. (1.4),

$$\frac{1}{\tau_s}=\pi f(\omega)\left(\frac{1}{T_{2G}}\right)^2\frac{\sum_{i\neq j}\,(a_\perp^{ij})^2}{\sum_{i\neq j}\,(a_\parallel^{ij})^2}, \tag{4.2}$$

where $\Sigma_{i\neq j}(a_\perp^{ij})^2/\Sigma_{i\neq j}(a_\parallel^{ij})^2\sim\{F_\perp(Q)/F_\parallel(Q)\}^4\sim 1/40$ in high-T_c cuprates. Among the materials we studied, τ_s should be shortest in Y1248 because of small NQR linewidth of 200 kHz $[f(\omega)=(4\pi\times10^5)^{-1}]$ and relatively large $1/T_{2G}\sim3\times10^4$ $\sec^{-1}$ near T_c. From these numbers, $1/\tau_s$ is estimated to be 56 $\sec^{-1}$.

In principle, such spectral diffusion could average out the oscillation of the magnetization distribution along the frequency axis with the period $2\pi/\tau$ in the stimulated echo experiments (Fig. 2). The characteristic time for this to occur is given by $(\pi/\tau)^2/D_\omega$. Even for the longest value of $\tau=5\times10^{-5}$ sec in our experiments, this characteristic time is of the order of 10^4 sec, which is many orders of magnitude larger than the range of T in our experiments (less than 10^{-2} sec). Therefore we conclude that the effect of the spectral diffusion is negligible.

We now consider the effect of fluctuations of the local field. Recchia *et al.* have considered the same problem for the ordinary spin-echo decay.[24] They assumed a Gaussian distribution for the accumulated phase and derived an analytic expression for the spin-echo decay in terms of the correlation function of the local field. Curro *et al.* applied this results to the case where the local field is given by Eq. (3.4) and I_z of a neighboring nuclear spin is fluctuating via the T_1 process.[6] This approach can be applied to the stimulated echo decay with only minor modification. If we assume a Gaussian distribution for the accumulated phase defined by Eq. (3.3), the stimulated echo intensity is given by

$$\left\langle\frac{1}{2}\cos\phi(T+\tau)\right\rangle=\frac{1}{2}\exp\left(-\frac{\langle\phi(T+\tau)^2\rangle}{2}\right). \tag{4.3}$$

As discussed in the Appendix, $\langle\phi(T+\tau)^2\rangle$ is the ensemble average of the contribution from individual neighboring nuclear spins. Each of them has to be distinguished whether it is a like nucleus, which is on resonance, or an unlike nucleus, which is off resonance. Thus if there are n types of unlike nuclei, we can write

$$\langle\phi(T+\tau)^2\rangle=P_0\langle\phi_{like}(T+\tau)^2\rangle+\sum_{i=1}^{n}\,P_i\langle\phi_{unlike,i}(T+\tau)^2\rangle, \tag{4.4}$$

where P_0 and P_i are the abundance of the like nuclei and ith unlike nuclei, respectively. In the Appendix, $\langle\phi_{like}(T+\tau)^2\rangle$ and $\langle\phi_{unlike,i}(T+\tau)^2\rangle$ are calculated as functions of T_{2G} of ^{63}Cu nuclei as defined in Eq. (1.4) and T_1's of like and unlike nuclei. In Fig. 6, T dependence of $\langle\phi_{like}(T+\tau)^2\rangle$ and $\langle\phi_{unlike}(T+\tau)^2\rangle$ are plotted for different values of T_{2G}/T_1 and τ/T_1.

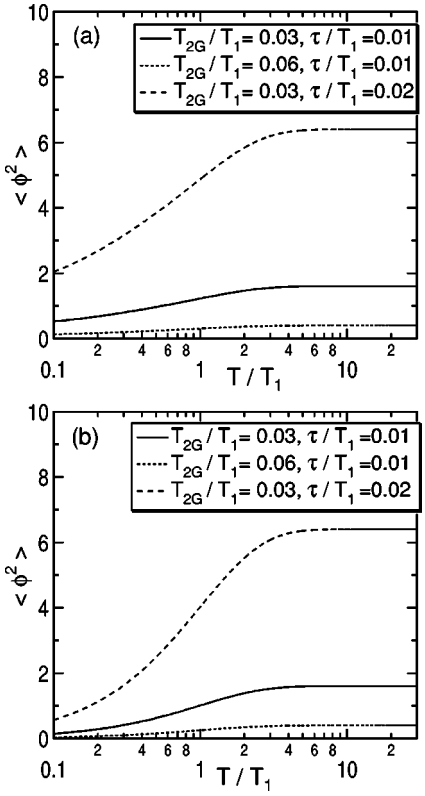

FIG. 6. The second moment of the accumulated phase $\langle \phi^2 \rangle$ as a function of T/T_1 for different values of T_{2G}/T_1 and τ/T_1 for (a) like-spin coupling and (b) unlike-spin coupling.

To summarize our analysis, we expect that the T and τ dependence of the stimulated echo intensity $M(T,\tau)$ is given by the product of the two decay process, i.e., the T_1 process and local-field fluctuations,

$$M(T,\tau) = M_0 \exp\left(-\frac{3T}{T_1}\right) \exp\left(-\frac{\langle \phi(T+\tau)^2 \rangle}{2}\right). \quad (4.5)$$

V. DISCUSSIONS

In this section we compare the experimental results with the calculation of Eq. (4.5). In order to examine the validity of our approach to analyze the local-field fluctuations, we separate the trivial T_1 process. In the following, we compare the stimulated echo intensity divided by $\exp(-3T/T_1)$, which we call the corrected intensity $M_{corr}(T,\tau)$, with the calculated results of $\exp(-\langle \phi(T+\tau)^2 \rangle/2)$. The results of comparison are shown in Figs. 7, 8, and 9.

A. Y-based compounds

We first discuss the results on underdoped $YBa_2Cu_4O_8$ and optimally doped $YBa_2Cu_3O_{7-\delta}$ (T_c=90 K). The full width at half maximum of ^{63}Cu-NQR spectra is about 200 kHz in these samples. Since almost all ^{63}Cu nuclear spins are excited by rf pulses for such a narrow spectrum, all ^{63}Cu spins are like nuclei and ^{65}Cu spins are the only unlike nuclei. Thus we set $P_0=0.69$ and $P_1=0.31$ in Eq. (4.4). In Fig. 7, the data for M_{corr} and the calculated stimulated echo decay curves are compared for Y1248 and Y1237 compounds. For calculation, we used the value of T_1 obtained from NQR

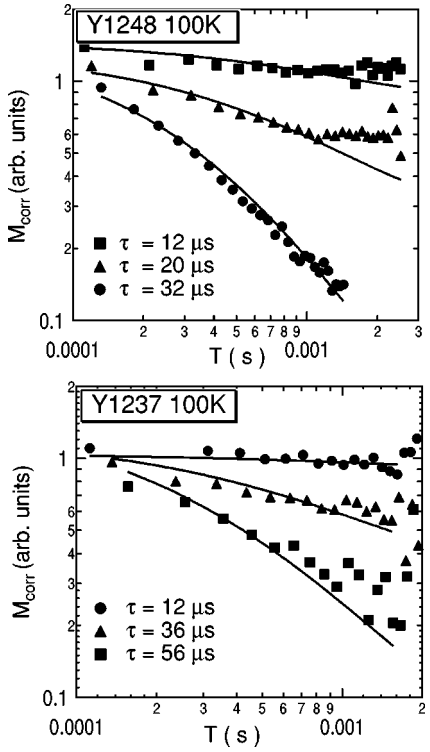

FIG. 7. The experimental stimulated echo decay M_{corr} (dots) is compared with the calculations (lines) for Y1248 and Y1237 at 100 K. We used the value of parameter T_{2G} given in Ref. 18.

inversion recovery measurements and the data of T_{2G} obtained by spin-echo decay measurements.[18] The overall magnitude M_0 is the only adjustable parameter in this comparison. The agreement between the experimental data and calculation is quite good. The calculation reproduces the ob-

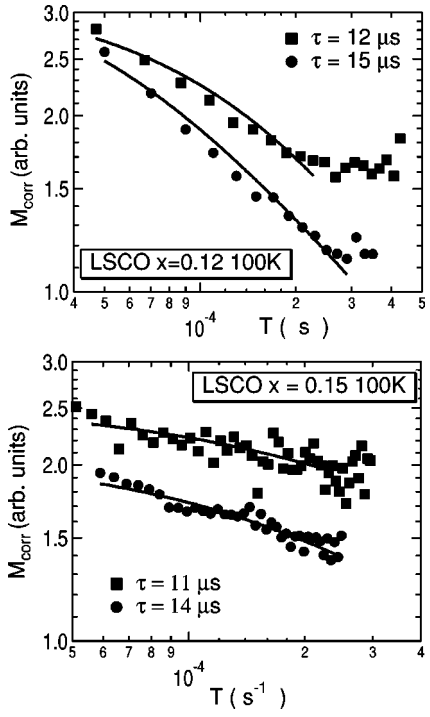

FIG. 8. The experimental stimulated echo decay M_{corr} (dots) and fitted curves based on Eq. (4.5).

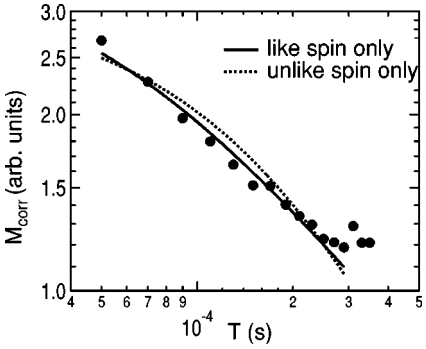

FIG. 9. The experimental data of M_{corr} for $x=0.15$ at 100 K (dots) are compared with two fitted curves, assuming 100% like-spin coupling (solid curve) or 100% unlike-spin coupling (dotted curve). The fitted values of T_{2G} are 25.0 [μs] for like-spin coupling and 26.7 [μs] for unlike-spin coupling.

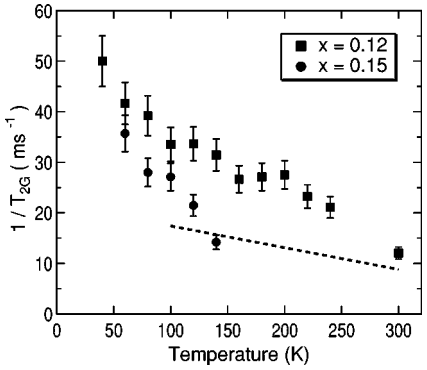

FIG. 10. Temperature dependence of $1/T_{2G}$ for LSCO $x=0.12$ and $x=0.15$ samples. The dotted line shows the results by Walstedt *et al.* (Ref. 26) for $x=0.15$ obtained from the spin-echo decay measurements using high-field NMR.

served change of behavior for different values of τ, in particular, the nonexponential decay for large values of τ is well explained by our model. Thus we believe that our model is valid for these materials.

B. $La_{2-x}Sr_xCuO_4$

As we mentioned before, the Cu-NQR spectra of LSCO show significant inhomogeneous broadening, whose full width at half maximum (FWHM) is about 2 MHz. Thus it is not possible to obtain $1/T_{2G}$ as defined in Eq. (1.4). On the other hand, Walstedt *et al.* measured the spin-echo decay rate using the $I_z=1/2\leftrightarrow -1/2$ center line of the ^{63}Cu NMR in the oriented powder sample in high magnetic field.[26] The FWHM of the NMR center line in LSCO is typically about 500 Oe. Although this is about four times narrower than that of Cu NQR, the whole region of the spectra cannot be excited by rf pulses. Moreover, the NMR spectra includes both the broad background from unoriented portion of the sample and the resonance from the so-called *B* site, which may affect the spin-echo decay measurements. Thus it would be important to obtain $1/T_{2G}$ by a different method.

Here we assume that our model for the stimulated echo decay is valid also for LSCO and extract the value of $1/T_{2G}$ by fitting the data of M_{corr} to $\exp(-\langle\phi(T+\tau)^2\rangle/2)$ with T_{2G} as a fitting parameter. The experimental data and fitted curves for LSCO are shown in Fig. 8. We used the value of T_1 determined from the inversion recovery technique.

There is minor ambiguity in this procedure. Since the ^{63}Cu NQR spectrum is so broad, only a fraction of ^{63}Cu spins is considered to be like nuclei. However, this is not a serious problem, since $\langle\phi_{like}(T+\tau)^2\rangle$ and $\langle\phi_{unlike}(T+\tau)^2\rangle$ are nearly identical for the range of parameters of our interest if the values of $1/T_1$ and γ_n are the same, as shown in Figs. 6 and 9. Based on the ratio between the NQR linewidth and the magnitude of the rf magnetic field of our experiments ($\sim$200 kHz), we chose rather arbitrarily that 10% of ^{63}Cu are like nuclei and 90% are unlike nuclei. The obtained value of $1/T_{2G}$ hardly depends on these numbers. We show in Fig. 9 two fits obtained by assuming that 100% of ^{63}Cu are like or unlike nuclei. The fitted values of T_{2G} differ only by 6%. Our analysis to determine T_{2G} is limited below 150 K for $x=0.15$ and below 250 K for $x=0.12$. At higher temperatures, where $1/T_{2G}$ gets smaller, T dependence of M_{corr} becomes too weak to determine $1/T_{2G}$ reliably. The values of T_{2G} thus derived are plotted against temperature for two samples, $x=0.12$ and $x=0.15$ in Fig. 10. $1/T_{2G}$ increase steeply as temperature decreases, similar to other high-T_c materials.[15,17,18] The results obtained by Walstedt *et al.* for $x=0.15$ between $T=100$ and 300 K using high-field NMR are also shown by the dashed line, after multiplied by $\sqrt{2}$ in order to take account of the difference between NQR and NMR measurements.[25,26]

Since the antiferromagnetic correlation is quite strong in high-T_c cuprates, we generally expect that the dynamic spin correlations obey some kind of scaling relation, which relates temperature dependence of various magnetic quantities to those of the antiferromagnetic correlation length ξ and the characteristic energy of the antiferromagnetic spin fluctuations ω_{sf}. These two quantities are related by the dynamical exponent z as $\omega_{sf}\propto\xi^{-z}$. The data of $1/T_{2G}$ and $1/T_1T$ have been used to extract the value of z in various high-T_c cuprates. It has been shown that if $\chi(Q)\propto\xi^2$,

$$\frac{1}{T_1T}\propto\omega_{sf}^{-1},\quad \frac{1}{T_{2G}}\propto\xi. \tag{5.1}$$

Therefore we expect T_1T/T_{2G}^z to be temperature independent.[27] While $z=1$ is expected at the quantum critical point (the boundary between Néel ordered states and disordered states) in two-dimensional quantum spin system,[28] antiferromagnetic spin fluctuations in itinerant electron systems is generally believed to be described by $z=2$.

Experimentally, the underdoped materials of the Y-based system, $YBa_2Cu_3O_{6.63}$ and $YBa_2Cu_4O_8$ show the $z=1$ behavior above T_s. Early data on the optimally doped $YBa_2Cu_3O_{6.9}$ are consistent with $z=2$.[27,29] However, recent ^{17}O-NMR experiments by Keren *et al.* pointed out importance of fluctuations of Cu nuclear spins due to both spin-lattice and mutual flip process in the analysis of the spin-echo decay data.[30] They obtained $z=1$ after correcting these effects.[30]

In Fig. 11, we plot the ratio T_1T/T_{2G}^z for $x=0.12$ and 0.15 against temperature with both $z=1$ and $z=2$. Apparently, the plot for $z=1$ is more temperature independent than the plot for $z=2$. Thus our results suggest the quantum critical

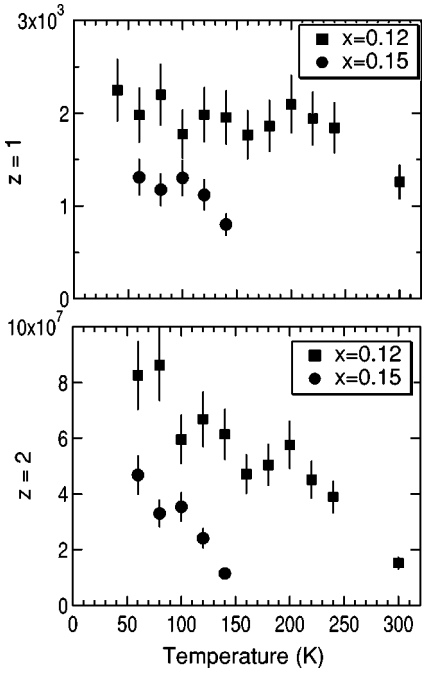

FIG. 11. The plot of T_1T/T_{2G}^z ($z=1$ or 2) in LSCO $x=0.12$ and 0.15 against temperature.

scaling for the magnetic excitations in underdoped LSCO. The results obtained by Walstedt *et al.* for $x=0.15$ between 100 and 300 K are also consistent with $z=1$.[26] To summarize our results on LSCO, consistent account of the stimulated echo decay data is given by our model using the values of $1/T_1$ measured by the inversion recovery technique, which show no clear signature of pseudo-spin-gap above T_c. The quantum critical scaling we found for LSCO is also consistent with the lack of spin gap, since such scaling breaks down in many of the underdoped cuprates below T_s. Why the spin gap is absent in LSCO is not fully understood. However, we speculate that it may be closely related to the instability toward the simultaneous spin and charge ordering found experimentally in LSCO.[31]

VI. CONCLUSION

We have applied the stimulated echo technique to the high-T_c superconductors by ^{63}Cu NQR. Our model assumes that the stimulated echo decay is caused by two dominant processes: the longitudinal T_1 relaxations and fluctuation of local field produced by longitudinal component of the nuclear spin-spin coupling. We argue that effects of spectral diffusion due to transverse component of the spin-spin coupling is negligible. We confirm that our model indeed gives good quantitative account of the experimental data for Y-based materials. We used the same model to deduce the value of $1/T_{2G}$ from the data of stimulated echo decay in LSCO. We found that $1/T_{2G}$ increases monotonously with decreasing temperature. The results show that the ratio T_1T/T_{2G}^z with $z=1$ is approximately independent of temperature, suggesting the quantum critical scaling in underdoped LSCO.

ACKNOWLEDGMENTS

We are grateful to Professor H. Yasuoka and Dr. Y. Itoh for suggesting stimulated echo experiments on high-T_c superconductors. One of the authors (S.F.) thanks S. Onoda for stimulating discussions. This work was supported by the Grant in Aid of the Ministry of Education, Sports and Culture. One of the authors (S.F.) thanks the JSPS for financial support.

APPENDIX

We calculate the second moment of the accumulated phase defined in Eq. (3.3), taking account of the fluctuation of the local field defined in Eq. (3.4) due to the T_1 process. We follow the approach formulated by Curro *et al.*[6] Since the values of I_{jz} is jumping among the four eigenvalues $\pm 3/2$, $\pm 1/2$, the local field is written as

$$h_i(t)=\frac{1}{\gamma_n}\sum_{j\neq i}\sum_m a_{\parallel}^{ij} m p_{jm}(t), \tag{A1}$$

where p_{jm} is a probability that I_{jz} takes the eigenvalue m. From Eqs. (A1) and (3.3), the second moment of the accumulated phase is given as

$$\langle\phi^2(T+\tau)\rangle=\left(\int_0^\tau\int_0^\tau-\int_0^\tau\int_T^{T+\tau}-\int_T^{T+\tau}\int_0^\tau+\int_T^{T+\tau}\int_T^{T+\tau}\right)\sum_{j\neq i}(a_{\parallel}^{ij})^2\sum_{m,m'}mm'\langle p_{jm}(t)p_{jm'}(t')\rangle dtdt', \tag{A2}$$

where we have assumed no correlation between different nuclear spins.

The time evolution of $p_m(t)$ is governed by the rate equation

$$\frac{dp_m(t)}{dt}=\sum_n W_{mn}p_n(t), \tag{A3}$$

$$\mathbf{W}=\frac{1}{2T_1}\times\begin{pmatrix}-3 & 3 & 0 & 0\\ 3 & -7 & 4 & 0\\ 0 & 4 & -7 & 3\\ 0 & 0 & 3 & -3\end{pmatrix}. \tag{A4}$$

We can write $\langle p_m(t)p_{m'}(t')\rangle=P_{mm'}(|t-t'|)/4$, where $P_{mm'}(t)$ is the probability that if a nuclear spin is in the state

m at the time t under the condition that it was in the state m' at $t=0$. $P_{mm'}(t)$ is equal to $p_m(t)$ obtained by solving the rate equation, Eq. (A3), with the initial condition that $p_{m'}=1$ at $t=0$. For instance,

$$P_{(3/2)(3/2)}(t)=\frac{1}{4}+\frac{9}{20}\exp\left(-\frac{t}{T_1}\right)+\frac{1}{4}\exp\left(-\frac{3t}{T_1}\right)+\frac{1}{20}\exp\left(-\frac{6t}{T_1}\right). \tag{A5}$$

We now have to consider the effects of three $\pi/2$ pulses, which redistribute the populations of like nuclear spins, which are on resonance. The rate equation, Eq. (A3), should be combined with the boundary conditions at $t=\tau$,

$$p_{3/2}(\tau^+)=p_{1/2}(\tau^+)=\frac{1}{2}[p_{3/2}(\tau^-)+p_{1/2}(\tau^-)], \tag{A6}$$

$$p_{-3/2}(\tau^+)=p_{-1/2}(\tau^+)=\frac{1}{2}[p_{-3/2}(\tau^-)+p_{-1/2}(\tau^-)], \tag{A7}$$

and the similar conditions at $t=T+\tau$. The rf pulses have no effect for unlike nuclear spins, which are off resonance.

Equation (A2) shows that $\langle\phi(T+\tau)^2\rangle$ is the sum of the contribution from individual neighboring nuclear spins. Therefore it is written as Eq. (4.4) according to the distribution of different types of like and unlike nuclei. We define $\phi_{like}(T+\tau)$ to be the accumulated phase for the hypothetical case where like nuclei occupy all the neighboring sites. Likewise $\phi_{unlike}(T+\tau)$ is defined to be the accumulated phase when all neighboring sites are occupied by ith unlike nuclei. They are calculated as

$$\langle\phi^2_{like}(T+\tau)\rangle=\frac{2}{0.69}\left(\frac{2T_{10}}{T_{2G}}\right)^2\left\{\frac{5}{4}\left[\frac{2\tau}{T_{10}}-2+2\exp\left(-\frac{\tau}{T_{10}}\right)\right]-\left[\frac{4}{5}\exp\left(-\frac{T-\tau}{T_{10}}\right)+\frac{1}{5}\exp\left(-\frac{6(T-\tau)}{T_{10}}\right)\right]\times\left[1-\exp\left(-\frac{\tau}{T_{10}}\right)\right]^2\right\} \tag{A8}$$

and

$$\langle\phi^2_{unlike,i}(T+\tau)\rangle=\frac{5}{2\times0.69}\left(\frac{2T_{1i}}{T_{2G}}\right)^2\left(\frac{\gamma_i}{\gamma_0}\right)^2\times\left[\frac{2\tau}{T_{1i}}+2\exp\left(-\frac{\tau}{T_{1i}}\right)-2+2\exp\left(-\frac{T}{T_{1i}}\right)-\exp\left(-\frac{T+\tau}{T_{1i}}\right)-\exp\left(-\frac{T-\tau}{T_{1i}}\right)\right]. \tag{A9}$$

Here $1/T_{2G}$ is the ^{63}Cu NQR spin echo decay rate as defined by Eq. (1.4), $1/T_{10}$ and $1/T_{1i}$ is the spin-lattice relaxation rate of like and ith unlike nuclei, and γ_0 and γ_i is the gyromagnetic ratio of like (^{63}Cu) and ith unlike nuclei, respectively. The result for $\langle\phi^2_{unlike,i}(T+\tau)\rangle$ has obtained by Recchia *et al.* previously.[32]

*Electronic address: fujiyama@kodama.issp.u-tokyo.ac.jp

[1] As reviews, *Physical Properties of High Temperature Superconductors*, edited by D. M. Ginsberg (World Scientific, Singapore, 1989), Vol. 1; *ibid.* (World Scientific, Singapore, 1990), Vol. 2; *ibid.* (World Scientific, Singapore, 1993), Vol. 3.

[2] As a review, *Strongly Correlated Electronic Materials*, edited by K. S. Bedell *et al.* (Addison-Wesley, Reading, 1994).

[3] T. Moriya, Prog. Theor. Phys. **16**, 641 (1956).

[4] H. Yasuoka, T. Imai, and T. Shimizu, *Strong Correlation and Superconductivity*, edited by H. Fukuyama, S. Maekawa, and A. P. Malozemoff (Springer-Verlag, Berlin, 1989).

[5] M. Takigawa, A. P. Reyes, P. C. Hammel, J. D. Thompson, R. H. Heffner, Z. Fisk, and K. C. Ott, Phys. Rev. B **43**, 247 (1991).

[6] N. J. Curro, T. Imai, C. P. Slichter, and B. Dabrowski, Phys. Rev. B **56**, 877 (1997); R. L. Corey, N. J. Curro, K. O'Hara, T. Imai, C. P. Slichter, K. Yoshimura, M. Katoh, and K. Kosuge, *ibid.* **53**, 5907 (1996).

[7] A. Goto, H. Yasuoka, K. Otzschi, and Y. Ueda, Phys. Rev. B **55**, 12 736 (1997).

[8] Y. Itoh, T. Machi, A. Fukuoka, K. Tanabe, and H. Yasuoka, J. Phys. Soc. Jpn. **65**, 3751 (1996); *ibid.* **67**, 312 (1998).

[9] M. H. Julien, P. Caretta, M. Horvatić, C. Berthier, P. Ségransan, A. Carrington, and D. Colson, Phys. Rev. Lett. **76**, 4238 (1996).

[10] S. Ohsugi, Y. Kitaoka, K. Ishida, G. Zheng, and K. Asayama, J. Phys. Soc. Jpn. **63**, 700 (1994); S. Ohsugi, Y. Kitaoka, K. Ishida, and K. Asayama, *ibid.* **60**, 2351 (1991).

[11] H. Yasuoka, Hyperfine Interact. **105**, 27 (1997).

[12] S. Fujiyama, Y. Itoh, H. Yasuoka, and Y. Ueda, J. Phys. Soc. Jpn. **66**, 2864 (1997).

[13] Y. Itoh, M. Matsumura, and H. Yamagata, J. Phys. Soc. Jpn. **66**, 3383 (1997).

[14] C. H. Pennington and C. P. Slichter, Phys. Rev. Lett. **66**, 381 (1991).

[15] M. Takigawa, Phys. Rev. B **49**, 4158 (1994).

[16] D. Thelen and D. Pines, Phys. Rev. B **49**, 3528 (1994).

[17] C. H. Pennington, D. J. Durand, C. P. Slichter, J. P. Rice, E. D. Bukowski, and D. M. Ginsberg, Phys. Rev. B **39**, 274 (1989).

[18] Y. Itoh, H. Yasuoka, Y. Fujiwara, Y. Ueda, T. Machi, I. Tomeno, K. Tai, N. Koshizuka, and S. Tanaka, J. Phys. Soc. Jpn. **61**, 1287 (1992).

[19] E. L. Hahn, Phys. Rev. **80**, 580 (1950).

[20] M. Weger, Ph.D. thesis, University of California, 1961.

[21] J. R. Klauder and P. W. Anderson, Phys. Rev. **125**, 912 (1962).

[22] C. P. Slichter, *Principles of Magnetic Resonance* (Springer-Verlag, Berlin, 1990).

[23] A. M. Portis, Phys. Rev. **104**, 584 (1956).

[24] C. H. Recchia, K. Gorny, and C. H. Pennington, Phys. Rev. B **54**, 4207 (1996).

[25] R. E. Walstedt and S-W. Cheong, Phys. Rev. B **51**, 3163 (1995).

[26] R. E. Walstedt and S-W. Cheong, Phys. Rev. B **53**, 6030 (1996).

[27] A. Sokol and D. Pines, Phys. Rev. Lett. **71**, 2813 (1993).
[28] A. V. Chubukov and S. Sachdev, Phys. Rev. Lett. **71**, 169 (1993).
[29] T. Imai, C. P. Slichter, A. P. Paulikas, and B. Veal, Phys. Rev. B **47**, 9158 (1993).
[30] A. Keren, H. Alloul, P. Mendels, and Y. Yoshinari, Phys. Rev. Lett. **78**, 3547 (1997).
[31] J. M. Tranquada, B. J. Sternlieb, J. D. Axe, Y. Nakamura, and S. Uchida, Nature (London) **375**, 561 (1995).
[32] C. H. Recchia, J. A. Martindale, C. H. Pennington, W. L. Hults, and J. L. Smith, Phys. Rev. Lett. **78**, 3543 (1997).